Available online at www.sciencedirect.com

ScienceDirect

Procedia Engineering 213 (2018) 374–382

Procedia Engineering

www.elsevier.com/locate/procedia

7th International Conference on Fatigue Design, Fatigue Design 2017, 29-30 November 2017, Senlis, France

Fatigue strength and weight optimization of threaded connections in tie-rods for aircraft structures

Markus Winklberger[a,*], Peter Heftberger[b], Mario Sattlecker[b], Martin Schagerl[a]

[a] *Institute of Structural Lightweight Design, Johannes Kepler University Linz, Austria*
[b] *RO-RA Aviation Systems, Schoerfling, Austria*

Abstract

Tie-rods are connecting elements used in an aircraft and they basically consist of a straight tube and two screwed in adapter ends. In order to optimize the tie-rod in terms of weight reduction a detailed knowledge of its fatigue strength is important. However, the complex load and contact distribution within the threaded connection between tube and adapter end make a secure and efficient fatigue design challenging. Moreover, the connection is realized with a thread insert to assure smooth adjustability of the adapter ends, which further increases the complexity of a fatigue strength assessment.

Thus, cyclic fatigue tests with a load ratio of $R = 0.01$ are performed to investigate the influences of thread insert length and position on the fatigue life of three different configurations. The experimental results are explained by Finite Element analyses using a detailed Finite Element model of the threaded connection. Finally microscopic examinations as well as the Finite Element analyses are utilized to further optimize the threaded connection in terms of reduced weight and high fatigue strength.

Peer-review under responsibility of the scientific committee of the 7th International Conference on Fatigue Design.

Keywords: Tie-rod; aircraft; threaded connection; thread insert; cyclic fatigue test; Finite Element simulation

1. Introduction

Tie-rods are commonly used connecting elements in an aircraft and attach, e.g., galleys, lavatories or storage bins to the fuselage structure. The specific design of tie-rods varies depending on the installation purpose and manufacturer. In this paper the threaded connection of interior tie-rods from RO-RA Aviation Systems is investigated. Fig. 1 shows a schematic sketch of such tie-rods with a straight tube and two adapter ends, which are screwed into the tube in order to adjust the length of the complete assembly. The threaded connection between the tube and the adapter end consists of two parts: a threaded sleeve and a screw insert in order to maintain a smooth-running connection to the adapter end. The sleeve is firmly attached to the tube. Such tie-rods are subjected to tension and compression loads with variable amplitude and must meet the high requirements of the aeronautic industry. Structural components in aircrafts in general have to be designed for a certain service life and therefore a detailed knowledge of their fatigue behavior is of great importance [1]. Furthermore, tie-rods have to meet weight requirements because of their large number in an aircraft. Previous fatigue tests carried out in the test facilities of the Institute of Structural Lightweight

*Corresponding author. Tel.: +43 732 2468 6677 ; fax: +43 732 2468 6662.
E-mail address: markus.winklberger@jku.at

1877-7058 © 2018 The Authors. Published by Elsevier Ltd.
Peer-review under responsibility of the scientific committee of the 7th International Conference on Fatigue Design.
10.1016/j.proeng.2018.02.037

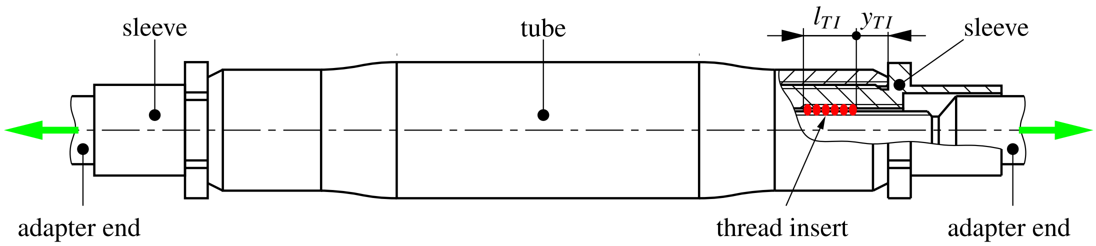

Fig. 1. Sketch of considered tie-rod to test influence of thread insert length and position on the fatigue life (not to scale)

Design have shown that the threaded connection between tube and adapter end is a critical failure location. Therefore, we performed detailed investigations in order to optimize the threaded connection in terms of both, increased fatigue strength and reduced weight.

Numerous influences on the fatigue life of threaded connections have already been investigated [2–4], considering the threaded connection as a standard bolt and nut. They also include conclusions regarding general threads but for the estimation of the fatigue life of threaded connections including thread inserts no explicit information was found in literature.

An analytical approach to calculate the fatigue strength based on nominal or local stresses is presented by the FKM guideline [5]. For threaded connections the FKM guideline refers to existing guidelines such as the VDI guideline 2230 [6], which is only valid for fastening threads. Therefore, both guidelines [5, 6] are also not applicable for the threaded connection given in tie-rods. Another approach is to apply the local concept in combination with Finite Element simulations to estimate the fatigue life of threaded connections [3, 7, 13]. Material properties such as the cyclic stress-strain curve and the strain life curve are inevitable input parameters for the local concept [4]. For the given tie-rod components these detailed material informations were not available to the authors. Additionally, the situation of two threads (one between tube and sleeve and the other between sleeve and adapter end) in close vicinity and their possible interdependence make a secure and accurate fatigue life estimation challenging.

Therefore, the influence of thread insert length l_{TI} and position y_{TI} (see Fig. 1) on the fatigue life is investigated experimentally by cyclic fatigue tests. Three considered configurations are listed in Table 1. Subsequently, the samples of the fatigue tests are analyzed by microscopic examinations of the crack location. Results of the fatigue tests were also compared to Finite Element simulations of the threaded connection.

Table 1. Three configurations to investigate the influence of the thread insert length and position.

	l_{TI} in mm	y_{TI} in mm
Configuration 1 (cfg1)	15	1
Configuration 2 (cfg2)	10	1
Configuration 3 (cfg3)	10	6

Nomenclature

cfg1-3	Configuration 1-3 of the threaded connection
l_{TI}	Length of thread insert (in mm)
y_{TI}	Position of thread insert (in mm)
S_a	Nominal stress amplitude (in MPa)
N	Cycles to failure
E	Young's modulus (in MPa)
ν	Poisson's ratio
n	Ramberg-Osgood exponent
$R_{p0.2}$	Yield strength (in MPa)
R_m	Ultimate strength (in MPa)
A	Elongation at fracture (in %)
ε	Strain (in m/m)
σ	Stress (in MPa)

2. Cyclic fatigue tests

Cyclic tests are performed to measure the fatigue life of three considered thread insert configurations. The tests are performed with three identical specimens per considered load level, in order to get a statistical measure of the results.

2.1. Test setup

The cyclic fatigue tests are performed on a test rig with an hydraulic cylinder. The utilized 100 kN cylinder is load controlled and a load ratio of $R = F_{min}/F_{max} = 0.01$ is defined for all fatigue tests. A test frequency of 10 Hz is used for all specimens except for tests with the highest loading, which were carried out at a frequency of 7.5 Hz due to cylinder performance. The utilized test rig is depicted in Fig. 2, where the hydraulic cylinder is connected to an alignment device in two test setups. In order to test both threaded connections of one specimen the complete assembly is tested with the setup one in Fig. 2a. After failure of one threaded connection the test is continued with the intact specimen end utilizing the second test setup (see Fig. 2b). In the first setup the complete specimen is mounted to the test rig with adapter ends having a threaded bolt on one end to hold the specimen and a fork shaped bolt connection on the other end to be fixed to the alignment device. Necessarily, in order to perform tests with the second test setup, the specimen had to be cut in the middle. Additionally the inner diameter was machined to fit precisely into the tube clamping device. In both setups the surrounding alignment device ensures the axial loading of the specimen.

2.2. Test results

Test results are represented by stress amplitude S_a and cycles to failure N. More specific S_a is the nominal stress amplitude in the tube at the threaded connection, where the nominal diameter of the tube's female thread and the outside diameter of the tube are considered for the cross section. All samples showed the same failure mode at the threaded connection, where the sleeve was pulled out after the tube cracked open in axial direction (see Fig. 2a). The results of the fatigue tests for the three different configurations (see Table 1) are given in Fig. 3. All measured data points are considered to be within the finite life fatigue strength regime, hence a linear regression of these data points is appropriate [5, 9, 10]. Comparing fatigue measurement data of configurations cfg1 and cfg3 shows a doubling of fatigue life time ratio. At the stress amplitude of $S_a = 65$ MPa, cfg3 even yields a 20 times higher fatigue life compared to cfg2. In order to understand these differences in fatigue lives a microscopic investigation of the cracks in the threaded connection after failure is done, followed by a Finite Element analysis.

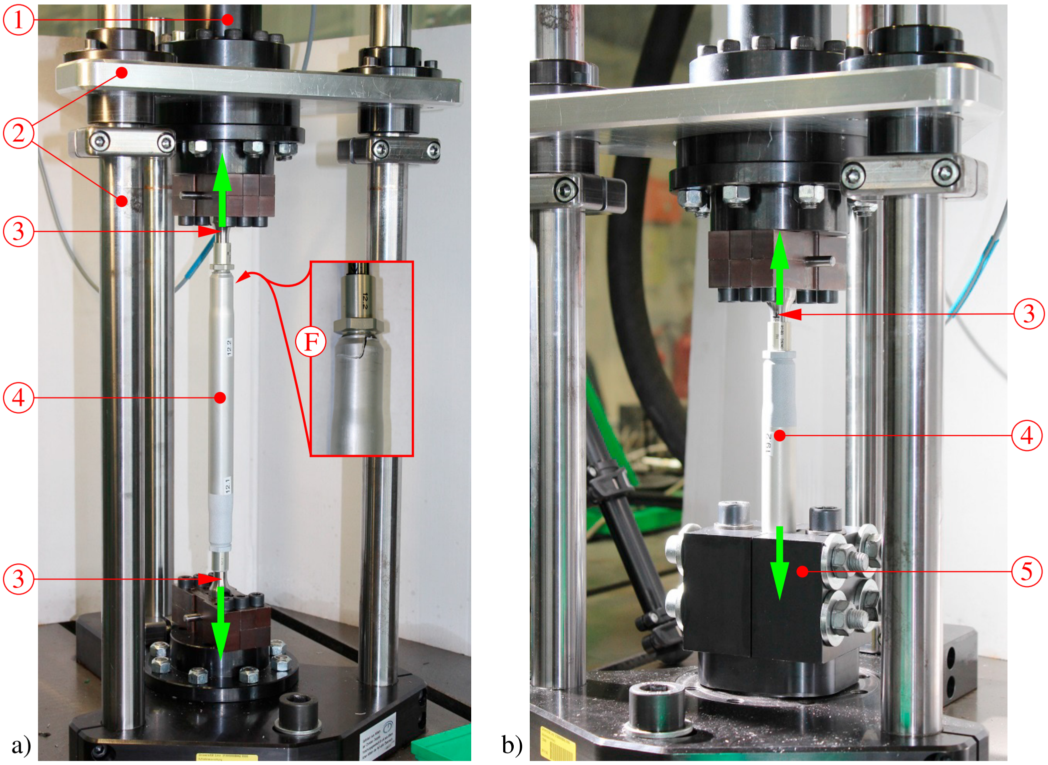

Fig. 2. Test rig and two setups for a) the whole specimen and b) the cutted specimen after failure of one end. Components are the hydraulic cylinder (1), alignment device (2), adapters (3), specimen (4), tube clamping device (5). All specimen showed the same failure mode at the threaded connection (F).

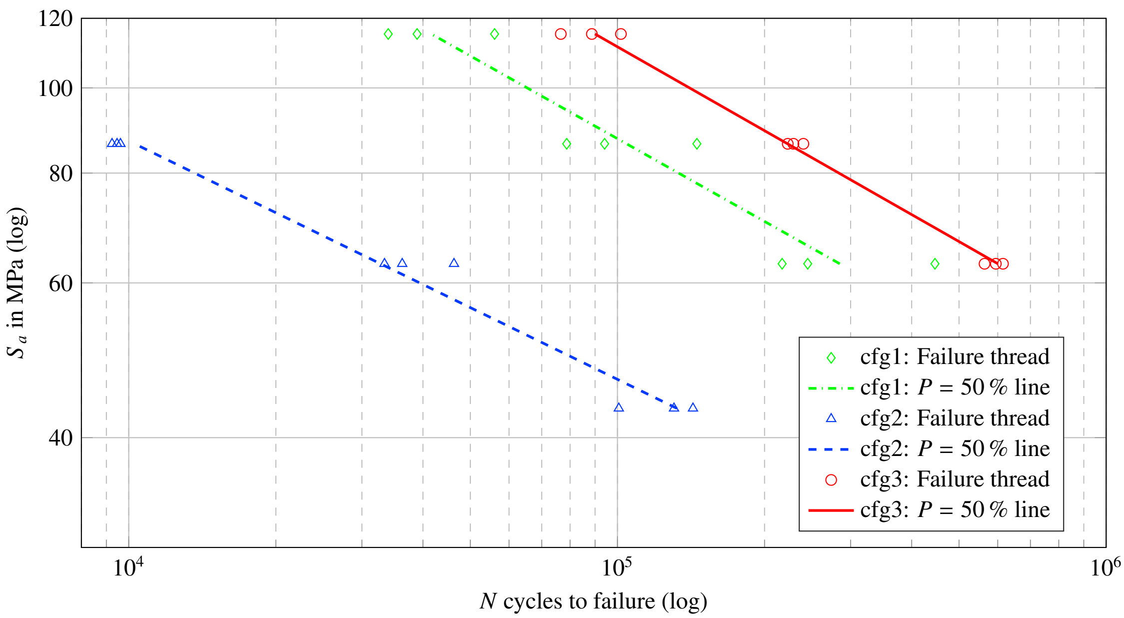

Fig. 3. Results of cyclic fatigue tests. The linear regression lines were calculated using a least squares fit algorithm by minimizing the squared distances in cycle direction as described in [8].

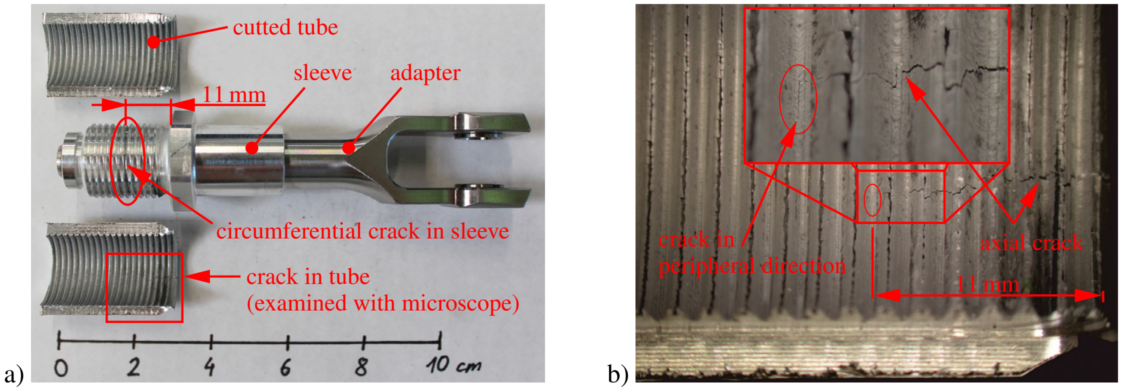

Fig. 4. Crack investigation with stereomicroscope Olympus SZX10, a) threaded connection cut open, b) crack in tube (female thread) with detail of crack tip.

2.3. Failure mode of threaded connection

As mentioned above, all specimen showed the same failure mode at the threaded connection at the tube ends where the sleeve is screwed in. One fatigue test with a specimen in cfg2 was stopped after a crack was already visible in the tube but before a complete failure of the threaded connection. This allowed to examine the failure mode of the threaded connection. To remove the tube while keeping the crack location as well as the sleeve intact a milling machine was used. The tube was cut twice in axial direction, each time 90° away from the visible crack. Fig. 4a depicts the tube and the sleeve after the cutting process, both with a clearly visible crack. The distance of the circumferential crack to the hexagonal part of the sleeve is approximately 11 mm. Furthermore, the tube with the crack was examined optically using a stereomicroscope. The microscopic picture of the female thread of the tube in Fig. 4b shows that the crack propagation direction changed from axial to peripheral also at the same position as the circumferential crack in the sleeve.

Following fracture mechanism of the threaded connection is proposed. At first the sleeve breaks at the end of the thread insert. Then the overloading of the tube end results in one or more cracks initiating at the open end of the tube. Subsequently, one or maximum two cracks get dominant and grow in axial direction. When the crack tip reaches the last thread turn of the thread insert, where the sleeve is already broken, the crack direction turns by 90°. We assume that this crack growth in peripheral direction only lasts for few cycles till the threaded connection between tube and sleeve finally fails. In order to support this assumptions Finite Element simulations are performed (see. Section 3).

3. Stress analysis

The stress analysis of the threaded connection was performed using the Finite Element software Abaqus 6.14. The developed Finite Element model is validated with strain measurements of static tests. Finally the stress distributions in the tube of the considered three configurations are compared in order to explain the fatigue test results.

3.1. Finite Element model

The threaded connection is idealized as a axisymmetric two dimensional Finite Element model shown in Fig. 5. According to the literature [3, 7, 11–13], two dimensional Finite Element models are commonly used for threaded connections. They are less expensive in calculation, less complex to mesh and give comparable stress results to 3D-models, although the thread pitch is not represented. For the mesh axisymmetric linear four node elements with reduced integration (CAX4R) are used. The meshing of the threads is based on the recommendations of Seybold [3]. Therefore, in all thread roots of the tube, sleeve and adapter end the mesh

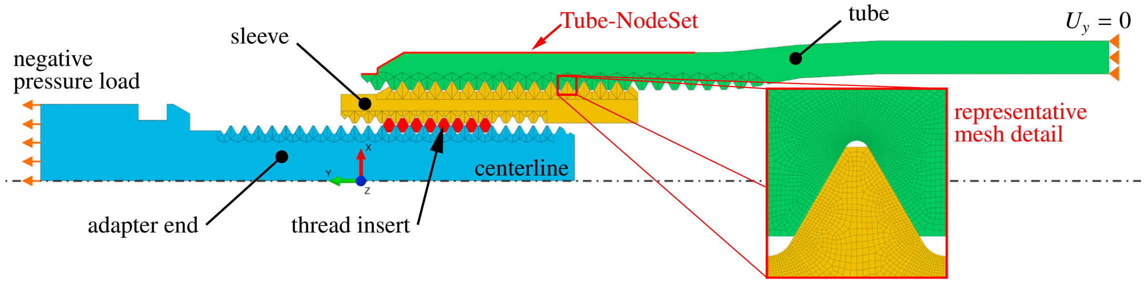

Fig. 5. Two dimensional Finite Element model with representative mesh detail of thread roots

size was set to fit at least 20 elements. A representative thread root and its mesh is given in Fig. 5. The contact definitions between adapter end and thread insert as well as thread insert and sleeve are modeled with frictionless tangential behavior and penalty normal behavior, see [14]. The contact between sleeve and tube is modeled with a friction coefficient of $\mu = 1.0$. The material properties of the tube, sleeve and adapter end are defined by the linear elastic and nonlinear plastic Ramberg-Osgood material model given by

$$\varepsilon = \frac{\sigma}{E} + 0.002\left(\frac{\sigma}{R_{p0.2}}\right)^n . \tag{1}$$

For the material of the thread insert a linear elastic and linear plastic material model is used, due to almost identical ultimate strength R_m and yield strength $R_{p0.2}$. The material parameters are given in Table 2. Load introduction and boundary conditions are depicted in Fig. 5, both at a sufficient distance from the threaded connection to prevent influences on the stress results used for the analysis (Tube-NodeSet).

Table 2. Material parameters used for the Finite Element model.

	E in MPa	ν	$R_{p0.2}$ in MPa	n	R_m in MPa	A in %
adapter end	196 600	0.27	1000	60	-	-
thread insert	118 000	0.27	890	-	900	5
sleeve	72 000	0.33	370	20	-	-
tube	73 000	0.34	315	12	-	-

3.2. *Validation of the Finite Element model*

In order to validate the developed Finite Element model strain measurements using a Digital Image Correlation system (DIC-system) were performed. During the measurements the specimen were loaded up to a nominal stress of 145 MPa in the cross section of the tube's thread. Fig. 6a shows the strain distribution at the tube end measured by the DIC-system. The measured strain in axial direction ε_{yy} along the red line (see Fig. 6a) is compared with the Finite Element results along Tube-NodeSet (see Fig. 5). Along the this path the simulation results and the measurement results are in good agreement for the three configurations. At the very end of the tube the strain measurements show a larger difference to the calculated paths. It is assumed that these deviations result from production tolerances and the neglected thread pitch in the two dimensional axisymmetric Finite Element model.

3.3. *Stress results*

Since the Finite Element model is validated, the stress results are analyzed in more detail. The experiments have shown that the different thread insert configurations influence the fatigue life of the threaded

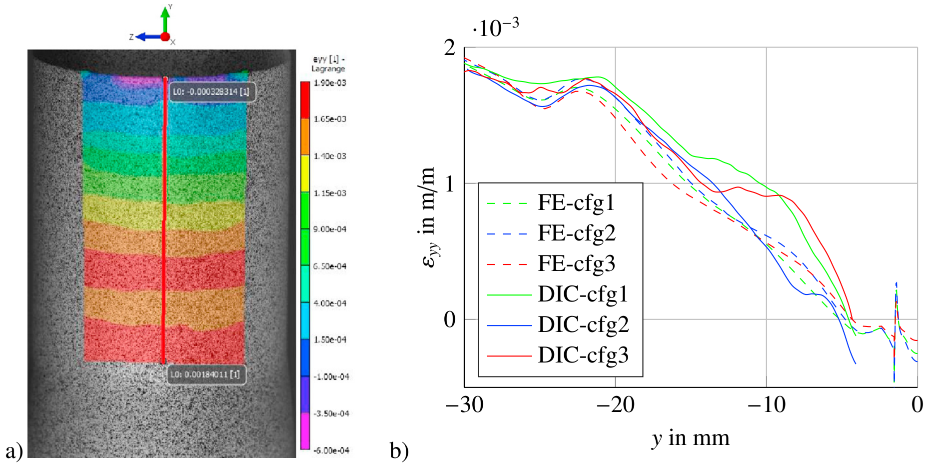

Fig. 6. Validation of Finite Element model a) DIC-measurement of tube (cfg2), b) Comparison of strains ε_{yy} along outside surface of tube (Tube-NodeSet) from FE-simulations and DIC-measurements.

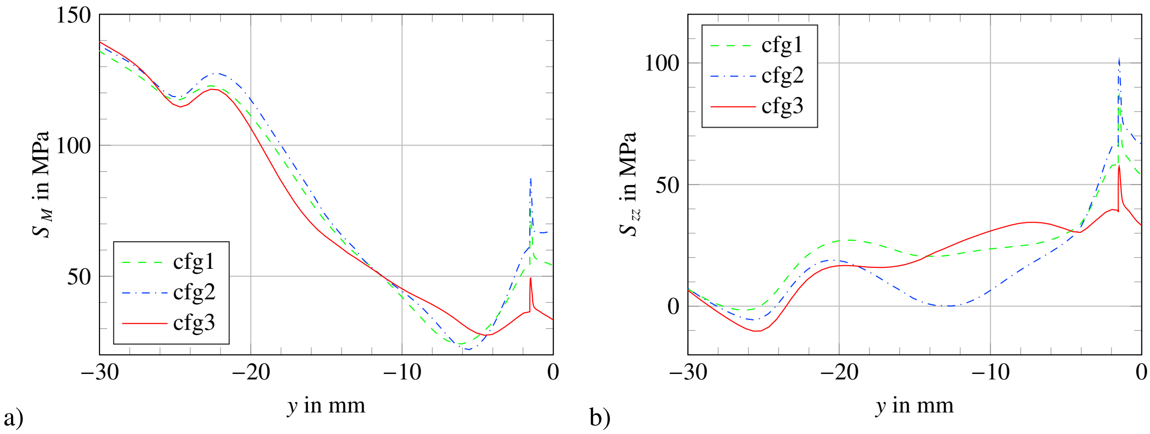

Fig. 7. Finite Element simulation results. a) Von Mises stress and b) hoop stress along outside surface of tube (Tube-NodeSet)

connection. The analysis focuses on the stresses in the tube to better understand the failure mode described in Section 2.3. All stress results were analyzed at the same loading which is equal to 145 MPa in the tube's thread cross section. Similar to the previous section the stresses along the red at the tube (Tube-NodeSet in Fig. 5) of the different configurations are compared. The von Mises stress and the hoop stress in peripheral direction are given in Fig. 7. Configuration cfg3 yields the lowest stress values in the first 5 mm of the tube for both kind of stresses. Additionally, in this part of the tube the hoop stress is almost identical to the von Mises stress, that results from the lack of thread engagement and hence no axial loading.

Therefore, we assume that the crack initiation at the open end of the tube (see Section 2.3) is mainly caused by hoop stresses. Furthermore, a comparison of the three considered configurations regarding their hoop stress distribution in the longitudinal section of the tube shown in Fig. 8, yields the same trend. The amplitude of stress concentrations at the open tube ends of the three considered configurations correlate with the fatigue test results. The hoop stress of cfg3 shows a much smoother distribution compared to the other two configurations, that results in a considerable longer fatigue life.

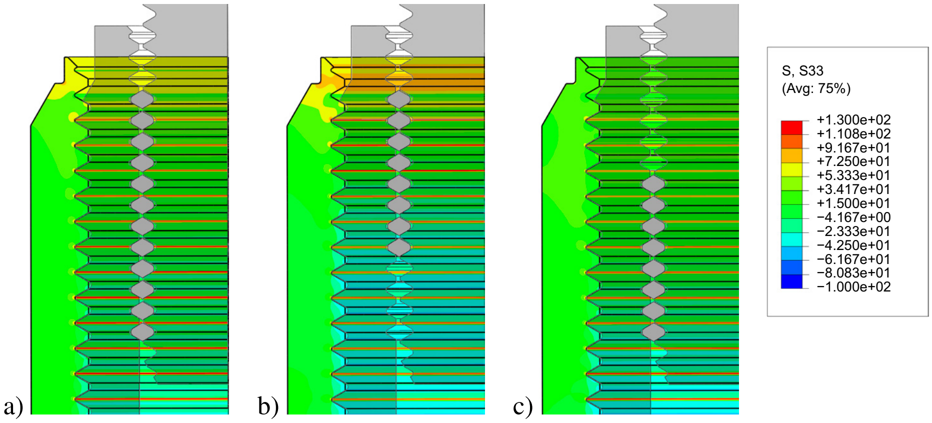

Fig. 8. Hoop stress distributions at a nominal axial tensile stress of 145MPa in the tube's thread. a) cfg1, b) cfg2, c) cfg3

4. Conclusions

In this study the fatigue lives of threaded connections within tie-rods were determined experimentally in order to optimize their design regarding fatigue strength and reduced weight. Three configurations with different thread insert lengths and positions were tested and compared. The configuration with the smallest thread insert length and deepest thread insert position showed the highest fatigue life (see Fig. 3). Our detailed numerical stress analysis showed that the hoop stress in the surrounding tube of the threaded connection is at the maximum, which may cause crack initiation and further lead to failure of the tie-rod. Comparing this stress concentration amplitude of the three different configurations with the fatigue life of the tested configurations supported our deliberations about the impact of stress concentrations at the open tube end on the fatigue life. Therefore, the stress concentration amplitude of the configuration with the highest fatigue life showed the lowest values at the open end of the tube (see Fig. 7 and Fig. 8c).

It is remarkable that the thread insert position of threaded connections in tie-rods has a bigger impact on the fatigue life than the thread insert length. Furthermore, the 10mm thread insert in the ideal configuration showed a higher fatigue life than the configuration with the 15mm thread insert. Therefore, an optimized design of the tie-rod may include a short thread insert, a reduced length of the sleeve and a more efficient design of the tube end to minimize the stress concentrations. The authors assume that all these measures can lead to a reduction of weight of the threaded connection and hence the complete tie-rod, without a decrease of fatigue strength.

Acknowledgements

The presented research work is financed by the Austrian Research Promotion Agency (FFG) within the initiative "Produktionsstandort OÖ 2050: Industrie 4.0". The authors thank Erich Humer for designing the test rig shown in Fig. 2 and his support in performing the fatigue tests.

References

[1] C.-C. Rossow, K. Wolf, P. Horst (Eds.), Handbuch der Luftfahrzeugtechnik, Carl Hanser Verlag München, 2014.
[2] W. Thomala, Beitrag zur Dauerhaltbarkeit von Schraubenverbindungen, Ph.D. thesis, TH Darmstadt, 1978.
[3] R. Seybold, Finite-Elemente-Simulation örtlicher Beanspruchungen in Schraubengewinden, Berichte aus der Werkstofftechnik, Shaker, 2006.
[4] R. Schneider, Örtliche Bewertung der Schwingfestigkeit von Gewindeverbindungen, Ph.D. thesis, TU Darmstadt, Institut für Werkstoffkunde, 2011.
[5] Rechnerischer Festigkeitsnachweis für Maschinenbauteile aus Stahl, Eisenguss- und Aluminiumwerkstoffen, FKM-Richtlinie, VDMA-Verlag GmbH, Frankfurt am Main, 2012.
[6] Systematische Berechnung hochbeanspruchter Schraubenverbindungen, VDI-Richtlinie 2230, VDI-Gesellschaft Produkt- und Prozessgestaltung, 2003.

[7] R. Schneider, U. Wuttke, C. Berger, Fatigue analysis of threaded connections using the local strain approach, Procedia Engineering 2 (2010).
[8] A. Martin, K. Hinkelmann, A. Esderts, Zur Auswertung von Schwingfestigkeitsversuchen im Zeitfestigkeitsbereich, Materials Testing 53.9 (2011) pp. 502–512.
[9] D. Radaj, M. Vormwald, Ermüdungsfestigkeit: Grundlagen für Ingenieure, Springer, Berlin, 2007.
[10] E. Haibach, Betriebsfestigkeit: Verfahren und Daten zur Bauteilberechnung, Springer, Berlin, 2006.
[11] J. W. Hobbs, R. L. Burguete, E. A. Patterson, Investigation into the Effect of the Nut Thread Run-Out on the Stress Distribution in a Bolt Using the Finite Element Method, Journal of Mechanical Design 125.3 (2003) pp. 527–532.
[12] J. Van Wittenberghe, J. De Pauw, P. De Baets, W. De Waele, M. A. Wahab, G. De Roeck, Experimental determination of the fatigue life of modified threaded pipe couplings, Procedia Engineering 2 (2010).
[13] D. Panic, T. H. Beier, M. Vormwald, Damage Assessment of Threaded Connections based on an Advanced Material Model and Local Concepts, Procedia Engineering 74 (2014).
[14] Abaqus 6.14 Online Documentation, Abaqus Analysis User's Guide, Dassault Systèmes, 2014.